Egyptian Journal of Chemistry

http://ejchem.journals.ekb.eg/

A Study Corrosion Properties by Magnetron Sputtered Nanocrystalline Al_2o_3 Thin Films

Muslim Idan Hamil[1*], Mohammed K. Khalaf [2], Mundher AL-Shakban[3]

1,3 Department of Physics, Faculty of Science, University of Misan, Maysan, Iraq.
2 Center of Applied Physics, Directorate of Materials Research, Ministry of Higher Education and Scientific Research /Science and Technology, Baghdad, Iraq.

Abstract

Titanium (Ti-6Al-4V) alloys had been mostly used for medical applications due to its good mechanical and chemical properties. This alloy tendency to emanate toxic aluminium (Al) and vanadium (V) due to their low corrosion resistance in body conditions. In this work, radiofrequency magnetron sputtering was used to prepare the Al2O3 thin films at different temperatures (400, 500, and 600oC) to increase the biocompatibility of Ti-6Al-4V alloy. The structure of the Al2O3 films was determined by the X-Ray diffraction (XRD) technique. The phases of Al2O3 thin films observed after heat treatment and its intensity phases increase at 600oC. The effect of depositing temperature on the microstructural morphologies of the thin films was studied by Field Emission Scanning Electron Microscope (FESEM). The particle size of the sputtered Al2O3 films ranged from 200 nm to 400 nm and was strongly influenced by annealing temperatures, the morphology of the films deposited before and after annealing has a characteristic agglomeration of particles. Potentiodynamic polarization analysis of the Al2O3 films confirms the inverse relationship between polarization resistance and corrosion current. The biocorrosion measurements for Al2O3 films deposited on the Ti-6Al-4V substrate in 3.5% NaCl solution have also been obtained. Clear improvement in the corrosion resistance was observed rather than for untreated, especially for thermally annealed (600oC) Al2O3 /Ti-6Al-4V samples. The corrosion rate was 0.356 mm/y for the uncoated sample, while 0.055 mm/y for Al2O3/Ti-6Al-4V in samples after annealing at 600oC. The average corrosion potential calculated was - 0.117 V. The results confirmed that coated alloys with 600°C thermally treated exhibited a better electrochemical behaviour compare with uncoated and non-thermally treated alloys possibly due to the better cohesion degree of the coatings.

Keywords: RF magnetron sputtering technique, Al2O3 thin films, Ti-6Al-4V alloy, simulated biological 3.5% NaCl solution and corrosion.

1. Introduction

Biomaterials are artificial materials such as metals, ceramics, composites, polymers, or natural materials that are utilized to replace missing or sick biological elements in implants, constructions, or joints. Due to their great strength and corrosion resistance, metal biomaterials are widely employed in medical applications in addition, stainless steel, Ti, magnesium, and Co-based alloys, among other metal biomaterials, have outstanding biomedical qualities. Biocompatibility is one of the best qualities of titanium and titanium-based alloys(1). Thin film coating has been increasingly important in a variety of technical and industrial applications in recent years. Because it combines common substrate characteristics (weight, flexibility, durability, thickness, absorbency, and transparency) with unique surface characteristics (2). Despite their superior bioactivity, biocomposites consisting of ceramics and polymers will never equal the strength and stability of metallic implants(3). Alumina (Al_2O_3) thin films have gained increasing interest in various industrial

*Corresponding author e-mail: muslim.iddan@uomisan.edu.iq; (Muslim Idan Hamil).

Receive Date: 23 February 2022; Revise Date: 21 March 2022; Accept Date: 29 March 2022.
DOI: 10.21608/ejchem.2022.123474.5522.

applications, ranging from optoelectronic devices, medical insets, and wear resistant coatings to catalysis applications, due to their excellent properties, such as wide bandgap, high transparency, large hardness, high wear resistance, excellent dielectric properties, and good chemical and thermal stability (4). The thermal expansion coefficient of Al_2O_3 is quite similar to that of Ti alloy; Ti alloy substrate thermal expansion coefficient is 8.7 10-6/K, while Al_2O_3 thermal expansion coefficient is 8.2 10-6/K. This resulted in a lower mismatch between the coated layer and the substrate, as well as the prevention of fracture formation when cooled from the evaluated temperature(5). Since alumina is an excellent insulator, a radio frequency (RF) alternating current has been used in many sorts of study for the formation of alumina thin films with deposition by magnetron sputtering. Because alumina is an excellent insulator, radio frequency (RF) alternating current is the best approach to employ in magnetron sputtering (6). The Ti-6Al-4V alloy is the most commonly used titanium alloy, and it was also the first titanium alloy to be recognized as an implant material under ASTM standards. Although titanium alloys have a variety of clinical qualities, this alloy has demonstrated corrosion susceptibility in both in vivo and in vitro circumstances. The corrosion aftereffects would result in the dissolution of V and Al ions, which would have negative consequences such as the development of Alzheimer's disease and cancer. Furthermore, one of the drawbacks limiting the use of titanium alloy has been its weak surface hardness(7). As a result, the goal of this research is to use a radiofrequency magnetron sputtering process to create a novel biocompatible and Al_2O_3 coating on Ti-6Al-4V alloy, as well as to explore surface characterisation, corrosion behavior, and hemocompatibility. In the present work, we used radiofrequency magnetron sputtering to study surface properties with the corrosion behavior of Ti-6Al-4V alloys. R F sputtering was used to explore these effects on the passive mechanisms of the Ti-6Al-4V alloys with respect to the surface conditions at the microstructure level.

2. Materials and Methods

Surface alteration of Ti-6Al-4V alloys by deposited biocompatibility of Al_2O_3. Using an RF magnetron sputtering technique and Ar gas, Al_2O_3 thin films were produced on Ti-6Al-4V alloy from Al_2O_3 targets. The Ti-6Al-4V samples were cut to a diameter of (20 mm x 20 mm), ground with 500 microns SiC grinding paper, and used as subtractions in a plasma sputtering system. The substrates were cleaned twice with ultrasonic in 96% ethanol (Sigma Aldrich, England), then distilled water for 15 minutes and dried in a discaiter at room temperature for 24 hours(ʌ) . The sputtering chamber was evacuated to a pressure of ($2*10^{-2}$) Torr before the sputtering gas (argon) was admitted. This was followed by a 15minute pre-sputtered operation to clean the target surface. As indicated in table, the deposition procedure was carried out with a fixed argon gas rate of ($5.5 *10^{-2}$) Torr, RF power of 150 W, chamber pressure of ($2 *10^{-2}$) Torr, and a deposition time of 1 hour (9). However, to examine the crystalline phase effect in the deposited thin films, the substrate temperature was changed from 400 to 600^{o}C. X-ray diffraction (Philips Geiger utilizing CuKa, =1.54 A0) was used to determine the structural parameters of Al_2O_3 thin films. The morphology of the films was observed using the FESEM (TESCAN MIRA3). ASTM G1-03/ASTM G102 was used to determine the corrosion process, and the corrosion behavior was evaluated by measuring the polarization curve (Tafel).

3. RESULTS AND DISCUSSION

3.1 X-Ray diffraction

Figure 1 shows the X-ray diffraction patterns of the samples before and after heat treatment at 400, 500, and 600^{o}C for 1 hour. There are four peaks that occur at 31.100, 39.220, 460, and 60.10, respectively, corresponding to (111), (222), (400), and (333) (10, 11) agreement with JCPDF code 21-1307(12). The planes' Bragg angles have moved to a new angle. The tetragonal Al_2O_3 phase was more clearly visible with planes (111), (107), (200), (222), (311), (400) and (401) on the XRD pattern of the thermally annealed films formed at 600^{o}C with deposition time 1h. (333)(13). Furthermore, as the annealing temperature is increased, the position of the peaks appears to alter. Shifting peaks are most likely caused by the release of inherent strain during the annealing process. The change of peak positions also suggests that the films are all under stress at the same time (10). Peak

brooding can arise as a result of changes in lattice structure in synthetic films. The thermal energy generated by annealing improves the mobility of active sites. Grain growth and flaw reduction during the annealing process are responsible for the increased mobility (14).

Table 1. Reactive RF sputtering conditions for depositing Al_2O_3 thin films.

Parameters	Values
Total pressure (Torr)	5×10^{-3}
Sputtering power (Watt)	150
The target to substrate distance (mm)	60
Substrates	Ti6AL4 V
Deposition time (hour)	1
Gas ratio (Ar)	Argon
Substrate temperature	373K

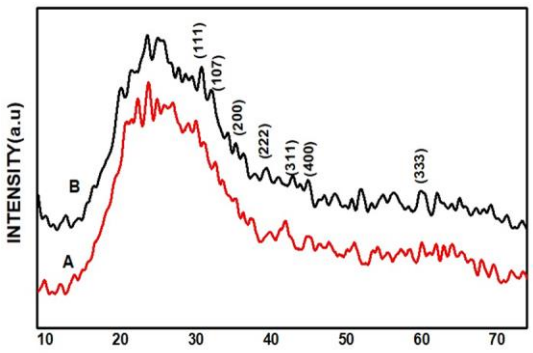

Figure (1): The X-ray diffraction of Al_2O_3 films deposited.

3.2. Surface morphology of the Al_2O_3 layers

Figure 2 (a – f) shows typical FESEM images of Al_2O_3 films formed under various deposition currents before and after annealing at 400, 500, and 600°C. Before heat treatment, amorphous particles and nonuniform clumping were found. Clusters were formed as a result of the particles agglomerating. The average particle size of Al_2O_3 as-deposited was found to be in the region of in the FESEM micrograph (25 nm). It was discovered that following annealing, the Al_2O_3 crystallite size increased, with the average particle size of Al_2O_3 coated at 400, 500, and 600°C increasing to 50, 50, and 70 nm, respectively. Increasing the annealing temperature (i.e., increasing the crystallinity of the film) supplies additional energy to the adatoms, resulting in increased microstructure order and particle size. However, an excessive supply of annealing temperature may cause the desired orientation to deteriorate, and the film will be bombarded with highly charged particles, resulting in internal film flaws (15).

3.3 Corrosion measurements

Various electrochemical techniques, such as potentiodynamic polarization, have been used to investigate corrosion behavior (Tafel analysis). When the open-circuit voltage is imposed on a metal sample, Tafel analysis is a well-established electrochemical technique that records the current. The polarization resistance (Rp), which is computed using Equations 1 and 2 (8), has an inverse relationship with corrosion current.

$$I_{Corr} = \frac{\beta_a \times \beta_c}{2.3\ R_p\ (\beta_a + \beta_c)} \qquad \text{(Eq. 1)}$$

Where, β_a = anodic Tafel slope, β_c= Tafel slope.

$$\text{Corrosion Rate (C.R)} = \frac{I_{corr} \times K \times EW}{d \times A} \qquad \text{(Eq. 2)}$$

K= constant that define the units of the corrosion rate = $3.272 \cdot 10^{-3}$ mm/(µA year), EW= equivalent weight (g/equivalent) = 11.768 g/eq., d = density (g/cm^3) = 4.420 g/cm^3, A = sample area (cm^2) = 0.151 cm^2.

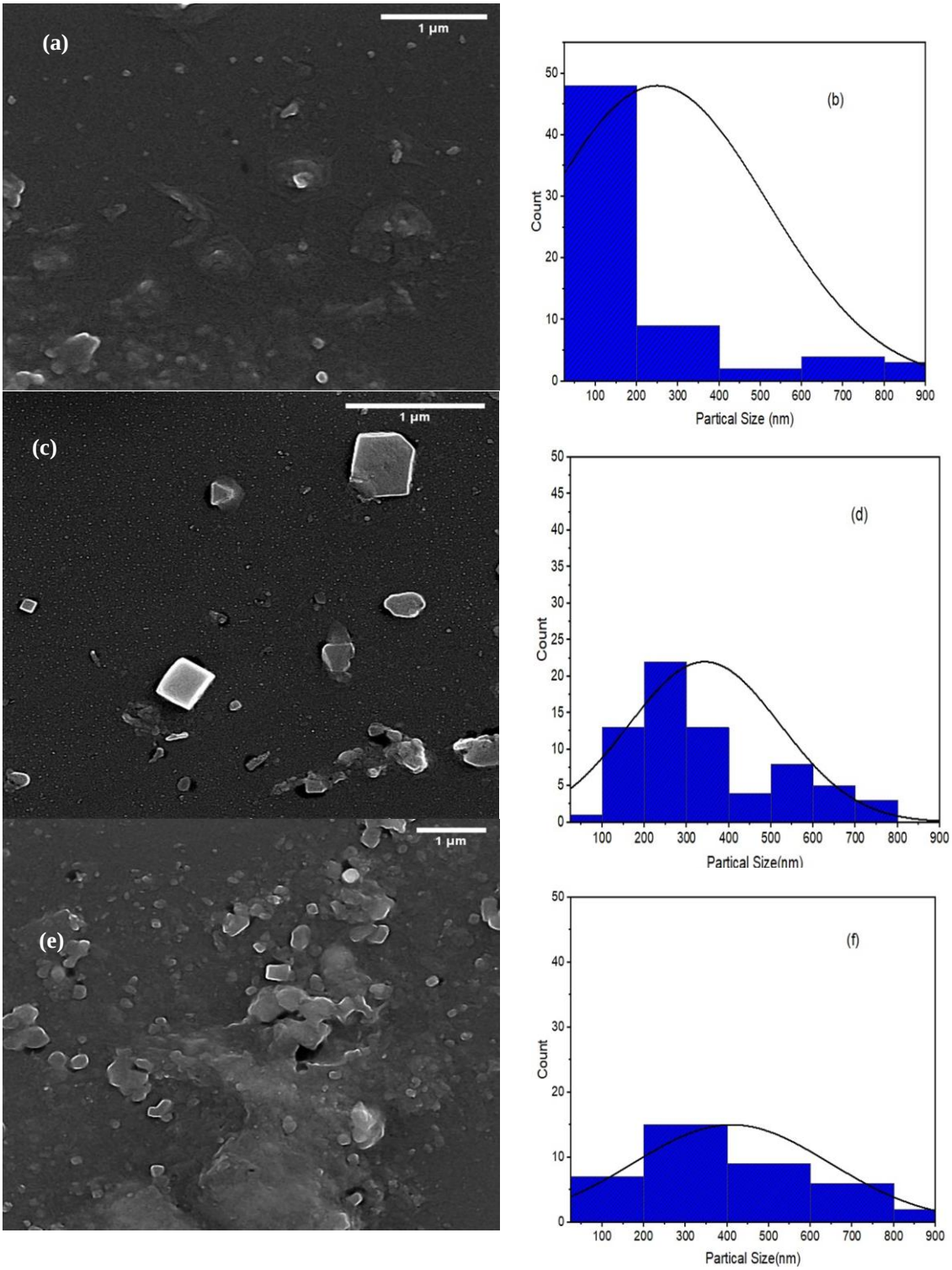

Figure (2). (a-b) FESEM image and histogram of Al_2O_3 film before annealing, (c-d) FESEM image and histogram of Al_2O_3 film coated at 400^oC, (e-f) FESEM image and histogram of Al_2O_3 film coated at 600^oC.

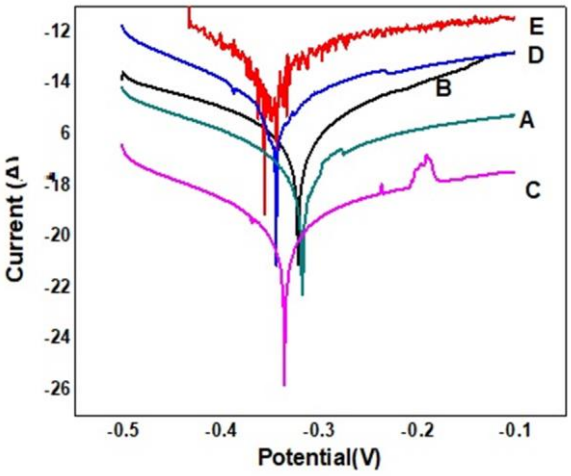

Figure (3): Polarization curves (Tafel) for Al_2O_3 films deposited on Ti-6Al-4V alloy by RF sputtering at 40 W for 1 hour. (A)Ti-6Al-4V alloy, (B) Al_2O_3 coated Ti-6Al-4V alloy (C) Al_2O_3 coated Ti-6Al-4V alloy at 400°C. (D) Al_2O_3 coated Ti-6Al-4V alloy at 500°C. (E) Al_2O_3 coated Ti-6Al-4V alloy at 600°C.

Figure 3 shows the polarization curve (Tafel) diagram for Al_2O_3 coated Ti-6Al-4V alloy (3). The average corrosion potential of the Ti-6Al-4V alloy when immersed in a simulated biological 3.5% NaCl solution (16-18) is - 0.317 V. For samples covered with Al_2O_3 before and after annealing, the corrosion potential migrated to the cathode side, with potential values of - 0.320, - 0.335, - 0.344, and -0.357 V, respectively.

Furthermore, by extrapolating the anodic and cathodic branches of the polarization curve to the corrosion potential, the corrosion current I_{corr} was determined from the polarization curves. Al_2O_3 films had corrosion currents of $2.5286*10^{-7}$ and $4.8088*10^{-8}$ A/cm^2 before and after annealing, respectively. In addition, when compared to Ti-6Al-4V alloy, the corrosion rate of coated samples was lower at 400, 500, and 600°C.

Another common technique for studying corrosion is open-circuit potential (OCP). The fluctuation of OCP with immersion time for Al_2O_3 coated Ti-6Al-4V alloy in 3.5% NaC% solution at 25°C is shown in figure (4). The initial OCP for untreated Ti-6Al-4V was – 12.74 V, and for the samples Al_2O_3 coated before and after thermal annealing, the potential steadily increased to – 7.731, - 3.794, and -1.993 V.

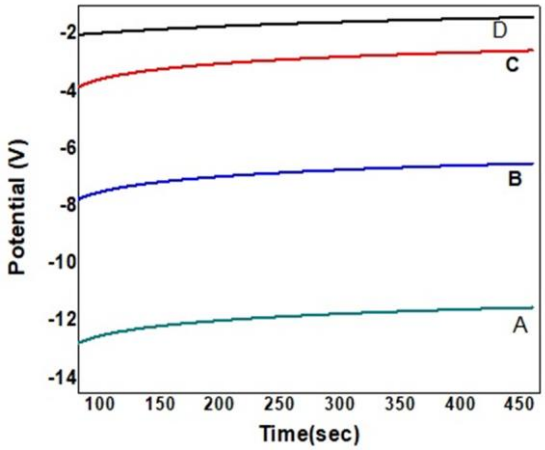

Figure 4. Open-circuit potential variation with time curve of Al_2O_3 coated on Ti-6Al-4V alloy by RF sputtering 40 W for 1 hour. (A)Ti-6Al-4V alloy,

Compared to the bare substrates, the coated samples demonstrate a positive shift in corrosion potential and a decrease in both corrosion current and corrosion rate values, as shown in table (2). With thermal annealing, a positive shift in corrosion potential is observed, as well as a decrease in both corrosion current and corrosion rate. The creation of a passive layer is responsible for these results.

4. CONCLUSIONS

Al_2O_3 films were successfully synthesized on Ti-6Al-4V alloy by RF-magnetron sputtering technique at high temperature, the coating of Ti-6Al-4V alloy with Al_2O_3 layer to improve the corrosion properties, such as the corrosion rate (Cor. Rate) and the polarization resistance (R_P). It has been observed that the particle sizes and corrosion properties were strongly influenced by temperature annealing, where the average particle size increased to 50 and 70 nm for the films heated at 400, 500, and 600°C. The corrosion rate of Al_2O_3 film deposited on Ti-6Al-4V substrate decreased, where it was 0.356 mm/year for uncoated sample while being 0.055 mm/year Al_2O_3 for the sample annealed at 600°C, this sample also presents the polarization resistance of 957.3 KΩ/cm^2, while it was 280.7 KΩ/cm^2 for the uncoated sample. All the coated samples and hear treatment appeared to be nobler in corrosion behaviors and decreased the value of corrosion values and current, meaning the TiO_2 coating has good protection for Ti-6Al-4V alloy in SBF and could be used in biomedical applications.

Table (2): Corrosion characteristics of Ti-6Al-4V samples coated with Al_2O_3.

Item	I_{corr}. Amp/cm^2	β_a (vol)	β_c (vol)	Corrosion potential (vol)	Corr.Rate (mm/y)	Rp KΩ/cm^2
Ti-Al-4V alloy	$3.0906*10^{-7}$	0.176	0.533	- 0.318	0.356	280.7
Al_2O_3 coated Ti-6Al-4V at 25^{0}C	$2.5286*10^{-7}$	0.976	0.587	- 0.323	0.292	574.9
Al_2O_3 coated Ti-6Al-4V at 400^{0}C	$1.4011*10^{-7}$	0.189	0.173	- 0.336	0.161	608.7
Al_2O_3 coated Ti-6Al-4V at 500^{0}C	$1.1458*10^{-7}$	0.145	0.351	- 0.346	0.132	744
Al_2O_3 coated Ti-6Al-4V at 600^{0}C	$4.8088*10^{-8}$	0.162	0.306	- 0.354	0.055	957.3

5. Conflicts of interest

"There are no conflicts to declare".

6. Acknowledgments

The authors would like to thanks to department of physics/ college of science - University of misan.

.

References

[1] Khorasani AM, Goldberg M, Doeven EH, Littlefair G. Titanium in biomedical applications—properties and fabrication: a review. Journal of biomaterials and tissue engineering. 2015;5(8):593-619.

[2] Pat S, Özen S, Şenay V, Aydoğmuş T, Elmas S, Korkmaz Ş, et al. A study on optical, morphological and mechanical properties of Al2O3 ultra-thin films deposited by RF reactive magnetron sputtering. International Journal of Surface Science and Engineering. 2015;9(5):415-24.

[3] Priyadarshini B, Rama M, Chetan, Vijayalakshmi U. Bioactive coating as a surface modification technique for biocompatible metallic implants: a review. Journal of Asian Ceramic Societies. 2019;7(4):397-406.

[4] Hao W, Marichy C, Journet C. Atomic layer deposition of stable 2D materials. 2D Materials. 2018;6(1):012001.

[5] Hamdi DA. Investigation the properties of hip implantation structure based on nanotechnology by using radio frequency magnetron sputtering. International Journal of Energy and Environment. 2017;8(6):515-22.

[6] Wei G, Ma P. Polymeric biomaterials for tissue engineering. Tissue Engineering Using Ceramics and Polymers: Elsevier; 2014. p. 35-66.

[7] Mthisi A, Popoola A. Influence of Al2O3 addition on the hardness and in vitro corrosion behavior of laser synthesized Ti-Al2O3 coatings on Ti-6Al-4V. The International Journal of Advanced Manufacturing Technology. 2019;100(1):917-27.

[8] Hamil MI, Siyah MA, Khalaf MK. http://ejchem. journals. ekb. eg. 2020.

[9] Sieniawski J, Ziaja W. Titanium alloys: advances in properties control: BoD–Books on Demand; 2013.

[10] Qiang W, Devarajan M. L. Variation of Structural and Surface Properties of RF Sputtered Aluminum Oxide (Al2O3) Thin Films Due to the Influence of Annealing Temperature and Time. IJMSA. 2014;3:404.

[11] Prins R. On the structure of γ-Al2O3. Journal of Catalysis. 2020;392:336-46.

[12] Lee J, Jeon H, Oh DG, Szanyi J, Kwak JH. Morphology-dependent phase transformation of γ-Al2O3. Applied Catalysis A: General. 2015;500:58-68.

[13] Jia S-k, Yong Z, Xu J-y, Jing W, Lei Y. Effect of TiO2 content on properties of Al2O3 thermal barrier coatings by plasma spraying. Transactions of Nonferrous Metals Society of China. 2015;25(1):175-83.

[14] Xiao D, Bao D-L, Liang X, Wang Y, Shen J, Cheng C, et al. Experimental and theoretical investigation of the control and balance of active sites on oxygen plasma-functionalized MoSe2 nanosheets for efficient hydrogen evolution reaction. Applied Catalysis B: Environmental. 2021;288:119983.

[15] Chen Q, McEwen GD, Zaveri N, Karpagavalli R, Zhou A. Corrosion resistance of Ti–6Al–4V with nanostructured TiO2 coatings. Emerging Nanotechnologies in Dentistry: Elsevier; 2012. p. 165-79.
[16] Dai N, Zhang L-C, Zhang J, Chen Q, Wu M. Corrosion behavior of selective laser melted Ti-6Al-4 V alloy in NaCl solution. Corrosion Science. 2016;102:484-9.
[17] Bodunrin MO, Chown LH, van der Merwe JW, Alaneme KK. Corrosion behaviour of Ti-Al-xV-yFe experimental alloys in 3.5 wt% NaCl and 3.5 M H2SO4. Materials and Corrosion. 2018;69(6):770-80.
[18] Bodunrin MO, Chown LH, van der Merwe JW, Alaneme KK. Corrosion behaviour of low-cost Ti–4.5 Al–x V–y Fe alloys in sodium chloride and sulphuric acid solutions. Corrosion Engineering, Science and Technology. 2019;54(8):637-48.